Materials and Design 31 (2010) 2942–2947

Contents lists available at ScienceDirect

Materials and Design

journal homepage: www.elsevier.com/locate/matdes

Effect of precipitation on post-heat-treated Inconel 625 alloy after friction stir welding

K.H. Song *, K. Nakata

Joining and Welding Research Institute, Osaka University, 11-1, Mihogaoka, Ibaraki, Osaka 567-0047, Japan

ARTICLE INFO

Article history:
Received 17 October 2009
Accepted 14 December 2009
Available online 21 December 2009

Keywords:
Welding (D)
Non-ferrous metal and alloys (A)
Microstructure (F)
Mechanical (E)

ABSTRACT

This study evaluated the mechanical properties of friction stir welded and post-heat-treated Inconel 625 alloy. Friction stir welding (FSW) was performed at rotation and traveling speeds of 200 rpm and 100 mm/min, respectively; heat treatment was carried out after welding at 700 °C for 100 h in vacuum. As a result, the application of FSW on Inconel 625 alloy led to the grain refinement in the stir zone, which resulted in increase in mechanical properties than those of the base material. Especially, applying heat treatment after FSW led to the improvement of mechanical properties of the welds; microhardness and tensile strength increased by more than 30% and 50%, respectively, as compared to FSW alone.

1. Introduction

Inconel 625 is a Ni-base superalloy strengthened by a solid solution of molybdenum and niobium in its nickel–chromium matrix; it retains high strength even at high temperature without any precipitation. This alloy has been used in aerospace applications, chemical power plants, and marine systems due to its superior properties; these include corrosion resistance, high strength, and creep resistance at high temperature [1]. Generally, the various joining methods on Ni-base superalloys, the fusion welding such as gas tungsten arc welding (GTAW), electron beam welding (EBW) and Laser beam welding (LBW), have been applied until now [2,3]. However, these welds limit the increase in mechanical properties due to the formation of a cast structure, which results from a higher heat input [2,3]. Friction stir welding (FSW) is a suitable technique to obtain excellent properties in the welds since FSW can be carried out in the solid state, which results in lower heat input as compared to fusion welding.

Precipitation plays an important role in improving the mechanical properties of Ni-base superalloys, such as hardness, strength, and creep rupture life [1]. Although Inconel 625 is a material strengthened by a solid solution, it is also affected by precipitates, such as MC system carbides and intermetallic phases formed at 550–750 °C [4–6]. In particular, the precipitation of gamma double prime (γ'') in the grains and $M_{23}C_6$ carbides in the grain boundaries has been reported to be effective in improving the mechanical properties [1]. However, the study of the precipitation of a friction stir welded Ni-base superalloys has not been reported thus far. Therefore, this study was carried out to evaluate the relationship between precipitation and the mechanical properties of heat-treated welds after FSW.

2. Experimental procedures

Inconel 625 alloy was used in this study; its chemical composition is given in Table 1. In order to carry out FSW, sheets of dimensions 150 mm × 32.5 mm × 2 mm were prepared. FSW was performed at a tool rotation speed of 200 rpm, a tool down-force of 42.1×10^3 N, and a traveling speed of 100 mm/min; a WC-Co tool was used with a shoulder 15 mm in diameter and a probe 6 mm in diameter and 1.8 mm in length. To obtain sound welds, the tool was tilted 3° forward from the vertical; argon gas was utilized to prevent surface oxidation during FSW. After FSW, to investigate the effect of precipitates on the mechanical properties, post heat treatment was carried out at 700 °C (heated up 10 °C/min from room temperature) for 100 h in vacuum of 1×10^5 torr; the samples were then cooled in the furnace from 700 °C to room temperature. A schematic for the post heat treatment is shown in Fig. 1.

To observe the macrostructures and microstructures in the welds, a solution of 15 ml HCl, 10 ml HNO_3, and 5 ml CH_3COOH was prepared, and the surfaces of the samples were etched after being polished with abrasive paper. To evaluate the dispersed MC system carbides in the microstructure, the scanning electron microscopy (SEM) and energy dispersive spectroscopy (EDS) analyses were employed. To evaluate the dispersed precipitates such as γ', γ'', and MC system carbides in the post-heat-treated specimens,

* Corresponding author. Tel./Fax: +81 6 6879 8668.
E-mail address: song@jwri.osaka-u.ac.jp (K.H. Song).

0261-3069/$ - see front matter © 2009 Elsevier Ltd. All rights reserved.
doi:10.1016/j.matdes.2009.12.020

Table 1
Details of chemical composition of Inconel 625 alloy.

Element	Ni	Cr	Fe	Mo	Nb	C	Mn	Si	S	Al	Ti
Mass (%)	61.28	21.99	3.24	9.0	3.53	0.017	0.1	0.09	0.001	0.18	0.32

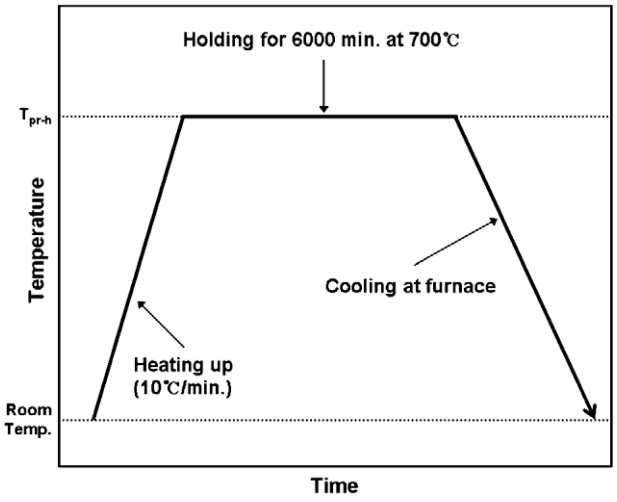

Fig. 1. Schematic of the post heat treatment cycle. T_{pr-h} indicates the temperature at which precipitation heat treatment was performed.

the transmission electron microscopy (TEM) analysis was employed. TEM observations were performed at an acceleration voltage of 200 kV. In case of the mechanical properties, Vickers microhardness and tensile tests were employed. Vickers hardness was carried out on the cross-section of the weld zone with a load of 9.8 N for a dwell time of 15 s. In the tensile tests, two types of tensile test specimens were used to evaluate the transverse tensile strength of friction stir welds and the longitudinal tensile strength of the stir zone, as shown in Fig. 2.

3. Results

The external shape and macrostructure of the welds are shown in Fig. 3. The material welded at a traveling speed of 100 mm/min showed sound weld properties without any defects on the surface, as shown in Fig. 3a. In the macrostructure, the material penetrated from the top to a depth of 1.5 mm without any defects in the welds; however, the band zone (indicated by arrow in macrostructure) was observed at the center of the stir zone, as shown in Fig. 3b. This was reported in studies on materials with high melting points, such as Ni-base superalloys [7–9]. Therefore, the band zone may have formed due to the high friction load between the material and the tool resulting from tool wear during FSW.

The results of SEM and EDS analyses on the band zone and normal stir zone are shown in Fig. 4. The band zone was at the center of the stir zone with a width of 50 μm, as shown in Fig. 4a. In the EDS result, an element (tungsten (W)) of the tool was detected in the band zone, as shown in Fig. 4b. However, in case of the normal stir zone, tool element (tungsten (W)) observed at the band zone was not detected, as shown in Fig. 4b. The temperature hysteresis is shown in Fig. 5. The temperature was measured at the backside of the plate at the center of the stir zone during FSW. The peak temperature was approximately 800 °C, which was reduced to 100 °C in 60 s, as shown in Fig. 5.

The microstructures of the welded material and post-heat-treated material are shown in Fig. 6. In the initial state, the base material consisted of grains, with grain sizes ranging between 5 μm and 15 μm, and MC system carbides such as NbC and (Ti, Nb)C were dispersed at the grain boundaries, as shown in Fig. 6a. In contrast, the stir zone showed a distribution of more refined grains as compared to the base material, with grain sizes ranging between 1 μm and 3 μm, and a dispersion of MC system carbides similar to that in the base material (Fig. 6b). In the post-heat-treated material, the base material showed coarser grains than those in the initial state, with grain sizes ranging from 5 μm to 25 μm (Fig. 6c). The post-heat-treated stir zone specimen also showed coarser grains, with grain sizes ranging from 3 μm to 5 μm, than those in the stir zone (Fig. 6d). Furthermore, in the post-heat-treated specimens, MC system carbides were also dispersed at the grain boundaries. The EDS

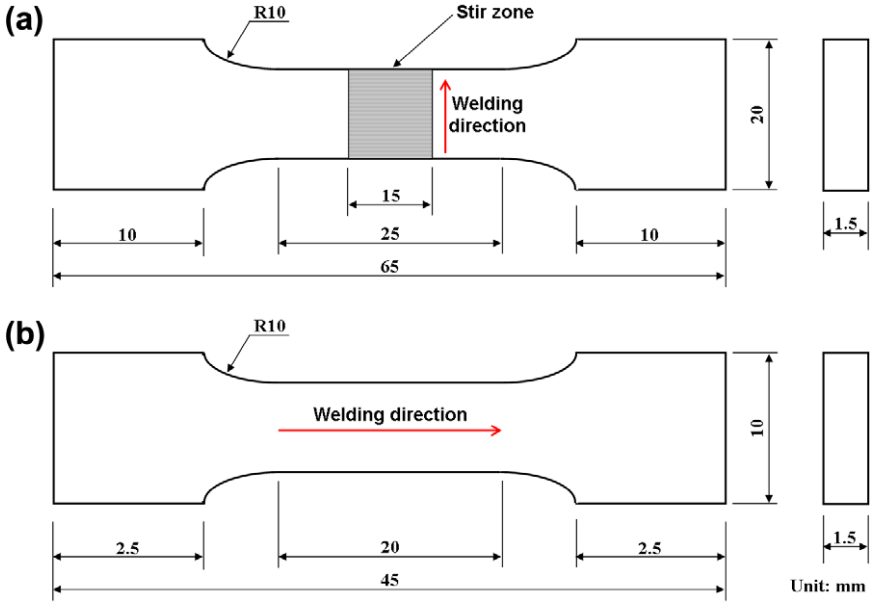

Fig. 2. Configuration of (a) transverse (weld joint) and (b) longitudinal (stir zone) tensile specimens used in this study.

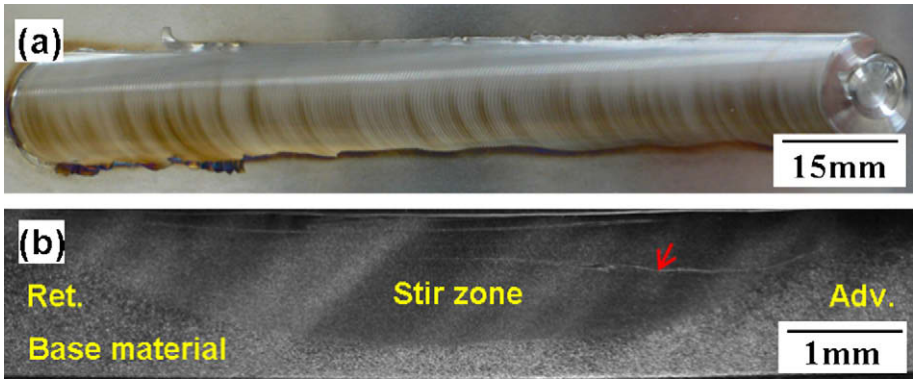

Fig. 3. (a) Top view and (b) macrostructure of friction stir welded Inconel 625. The arrow indicates the band structure in the stir zone.

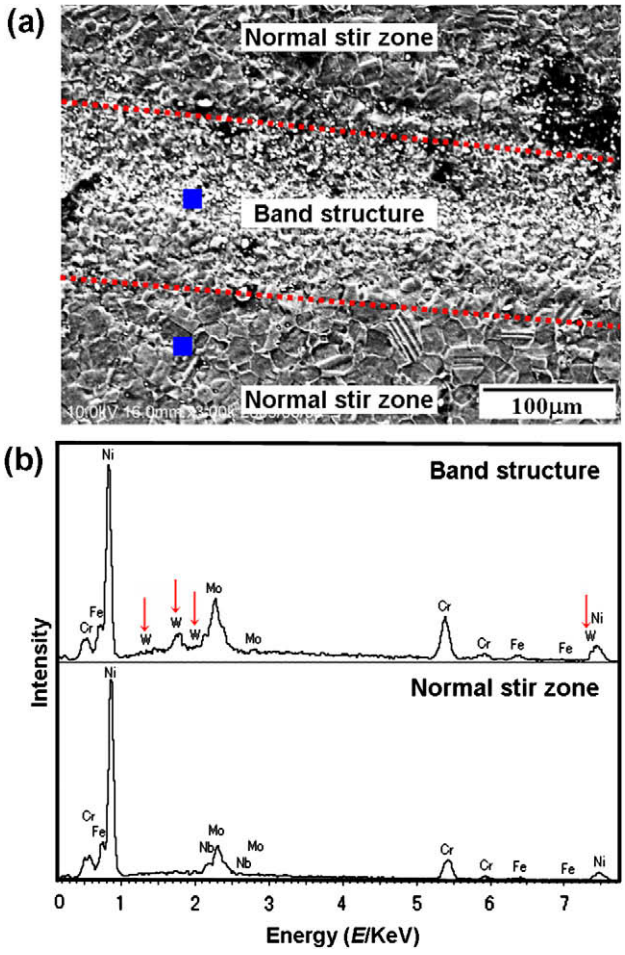

Fig. 4. (a) SEM image and (b) EDS spectra obtained from band structure.

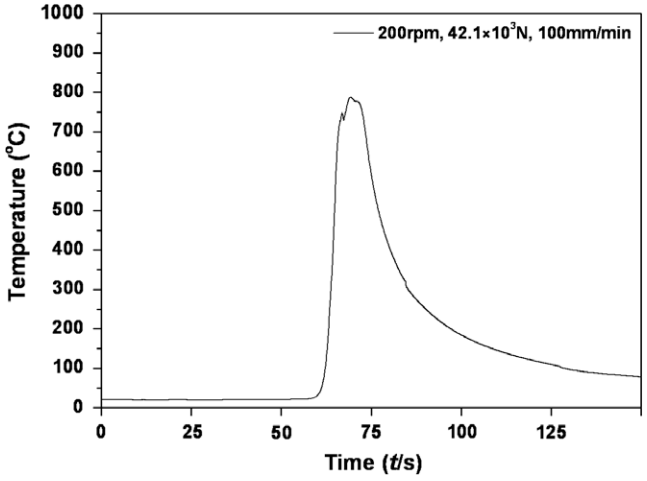

Fig. 5. Temperature hysteresis in stir zone during friction stir welding.

results for the MC system carbides observed in the microstructures are shown in Fig. 6e.

The images and selected area diffraction patterns of the post-heat-treated material are shown in Fig. 7. In the base material after the post heat treatment, precipitates such as $M_{23}C_6$ carbides and Ni_3Nb (γ'') were dispersed at the grain boundaries and in the grains with sizes of 40–80 nm. In the stir zone after the post heat treatment, many precipitates such as Ni_3Nb (γ'') and M_6C carbides were also present with particles sizes of 20–80 nm. Furthermore, in the case of the stir zone, more precipitates were formed in the grains than at the grain boundaries.

The change in microhardness due to post heat treatment is shown in Fig. 8. For friction stir welds, the Vickers microhardness of the base material ranged from 250 Hv to 300 Hv; however, the stir zone showed a significantly increased microhardness than that of the base material, ranging between 350 Hv and 390 Hv. In the case of the friction stir welds after the heat treatment, the microhardness increased to 350–400 Hv in the base material and 420–460 Hv in the stir zone.

Top views of the tensile tested specimens are shown in Fig. 9. At the initial state, the base material was elongated over the entire gage length and fractured at the center of the specimen, as shown in Fig. 9a. However, the welded material (transverse direction) was first deformed at the base material and fractured, as shown in Fig. 9b. For the heat-treated material after FSW, the base material was also elongated and fractured, similar to the welded material, as shown in Fig. 9c. The stir zone specimens (welded and post-heat-treated materials) also showed an elongated and fractured shape, as shown in Fig. 9d and e.

The tensile test results for the welded and post-heat-treated materials are shown in Fig. 10. The base material exhibited an ultimate tensile strength (UTS) of 943 MPa and elongation of 58%. FSW application led to the increase in strength; as a result, the UTS of the FSW joint specimen slightly increased to 1019 MPa, while its elongation decreased to 34%. In the FSW stir zone, the UTS was 1152 MPa, which is significantly higher than that of the base material, with an elongation of 35%. Post heat treatment on the welded material led to further increase in strength; the FSW joint specimen that was heat treated at 700 °C exhibited a UTS of 1164 MPa with an elongation of 20%. In case of the post-heat-treated FSW stir

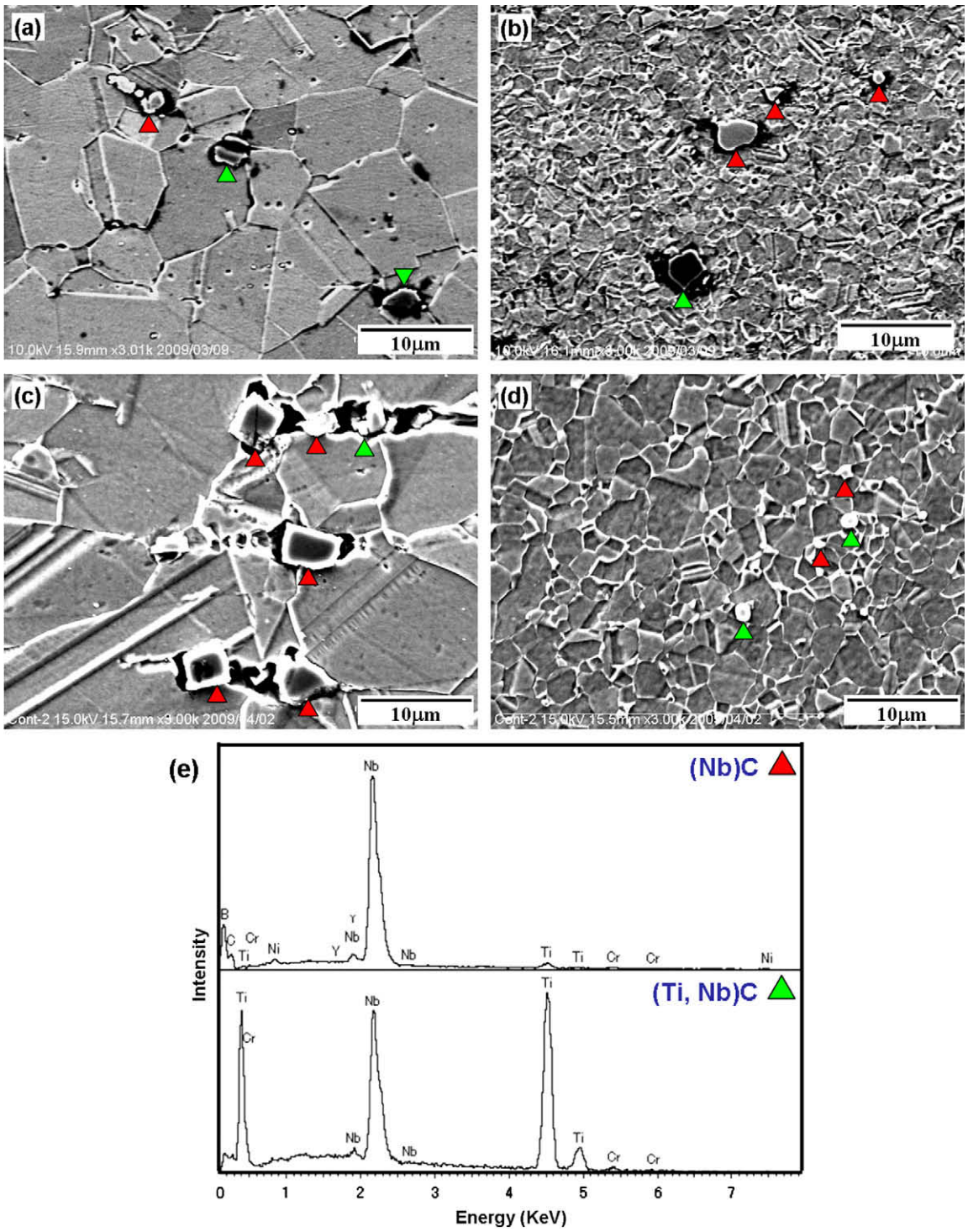

Fig. 6. (a–d) SEM images and (e) EDS spectra obtained from friction stir welded material and post-heat-treated material. Friction stir welded material: (a) base material and (b) stir zone. Post-heat-treated material: (c) base material and (d) stir zone.

zone specimen, the UTS increased more than that of any other specimens; the UTS was 1475 MPa, while the elongation slightly decreased to 18%.

4. Discussion

4.1. Grain refinement due to FSW

FSW of Inconel 625 alloy led to notable grain refinement in the stir zone. As a result, the grain size is significantly refined from 5 μm to 15 μm in the base material to 1–3 μm in the stir zone, as shown in Fig. 6a and b. This can be explained by the stored energy due to the severe deformation and the friction heat generated between the tool and the material during FSW. In other words, the material easily undergoes dynamic recrystallization due to the high strain rate (large stored energy) and friction heat during FSW. Furthermore, the peak temperature measured at the center of stir zone was 800 °C, which is sufficient for the recrystallization in Inconel 625 alloy. Further, the material perfectly cooled to 100 °C in 60 s, which prevents grain growth after recrystallization,

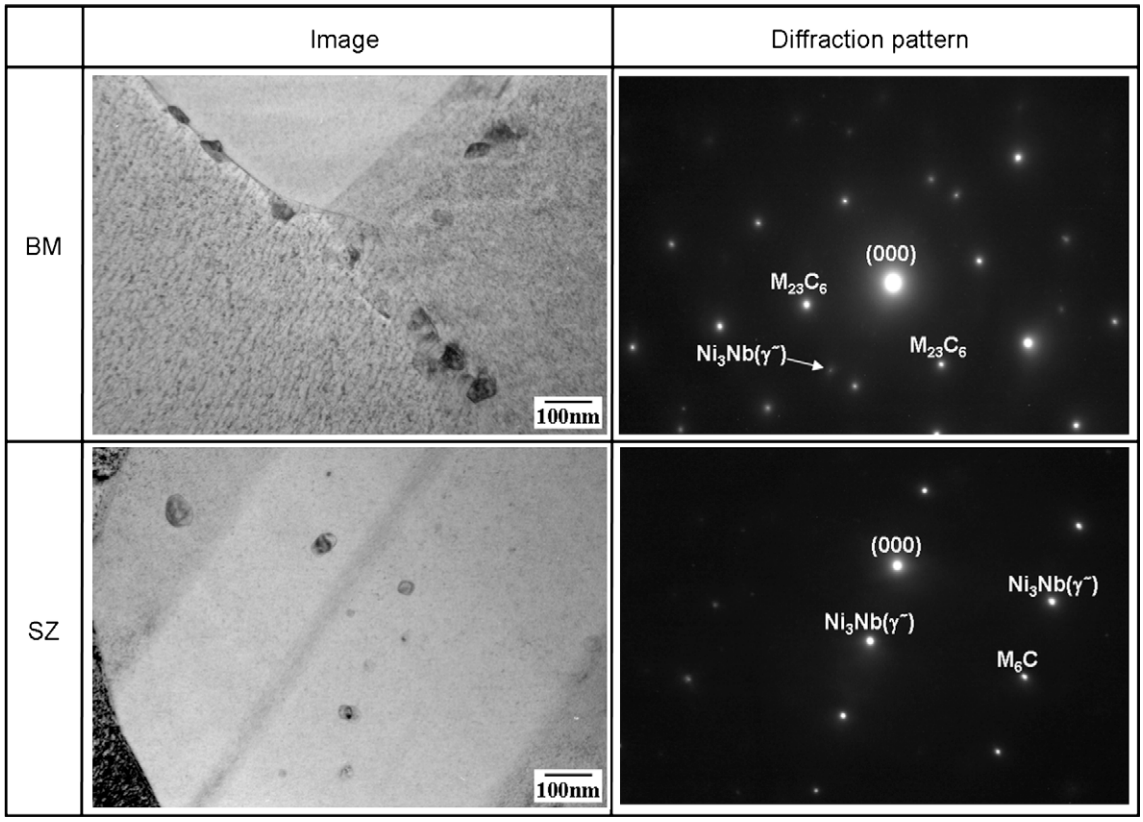

Fig. 7. TEM images and selected area diffraction patterns observed in post-heat-treated specimens. BM and SZ indicate the base material and stir zone, respectively.

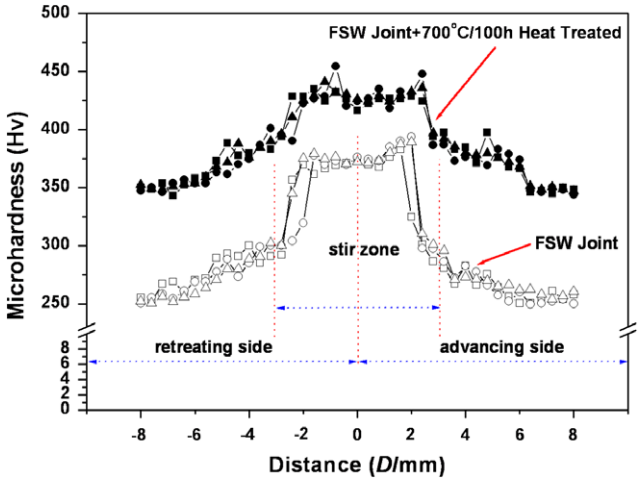

Fig. 8. Vickers micro hardness distribution in friction stir welded material and post-heat-treated material.

as shown in Fig. 5. Therefore, along with the high strain rate, sufficient heat input and fast cooling during FSW can lead to grain refinement more easily.

Inconel 625 alloy was used in this study; it has a lower stacking fault energy of fcc metals as compared to Al alloys [10]. The material with a lower stacking fault energy undergoes dynamic recrystallization more easily than materials with high stacking fault energy since recrystallization nuclei are readily formed, while it is difficult for the dislocations to be rearranged [11]. Further, FSW application is accompanied by a higher dislocation density and friction heat due to the severe deformation; this results in the promotion of recrystallized nucleation. As a result, the recrystallization nuclei are formed in the grains and at the grain boundaries, which coincidentally have a higher density of dislocations. Therefore, grain refinement can be achieved easily by employing FSW.

4.2. Improvement of mechanical properties due to FSW

The application of FSW on the Inconel 625 alloy led to the improvement of the mechanical properties of the welds, such as microhardness and tensile strength, due to grain refinement. As a result, the microhardness increased from 250 Hv to 300 Hv in the base material to 350–390 Hv in the stir zone due to the refined grains, as shown in Fig. 8. At the joints, the base material part in the specimen deformed first as compared to the welded zone and fractured, as shown in Fig. 9. This can be attributed to the grain refinement in the stir zone. In other words, the fracture in the base material was brought about by the distribution of coarsened grains, which resulted in low strength as compared to the stir zone. Further, the tensile strength of the stir zone specimen increased by more than 20% as compared to the base material, as shown in Fig. 10. Therefore, these results correctly show the relationship between the grain size and the mechanical properties of the welds.

4.3. Effect on precipitation due to post heat treatment

The Inconel 625 alloy used in this study is strengthened by a solid solution of molybdenum and niobium in its nickel–chromium matrix; however, it is also affected by precipitation at elevated temperatures [1,12]. Precipitation due to heat treatment in Ni-based superalloys has a notable effect on the mechanical properties [13–15]. In particular, the formation of precipitates such as γ' and γ'' in the Inconel 625 alloy is good for the yield, tensile, and creep rupture strength [1]. For MC system carbides such as MC, M_6C, and $M_{23}C_6$, the shape distributed at grain boundaries

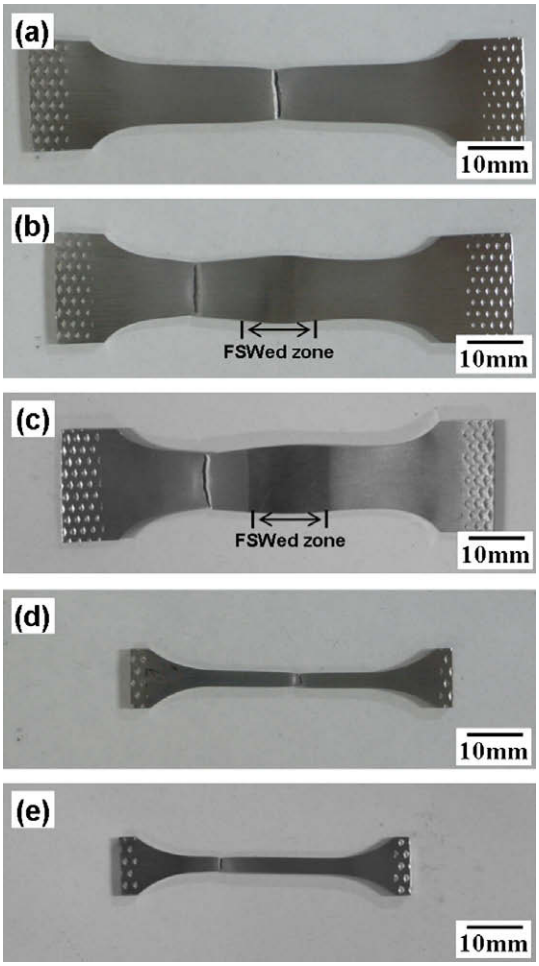

Fig. 9. Top views of specimens subjected to tensile tests. Transverse directions: (a) base material, (b) FSW joint, and (c) post-heat-treated specimen. Longitudinal direction: (d) FSW stir zone and (e) post-heat-treated FSW stir zone.

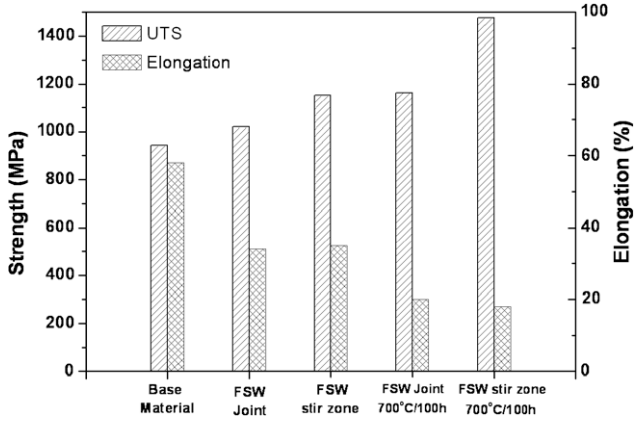

Fig. 10. Transverse (weld joint) and longitudinal (stir zone) tensile properties of friction stir welded materials and post-heat-treated material.

can affect the mechanical properties [13–15]. In this study, MC system carbides such as M_6C and $M_{23}C_6$ in the post-heat-treated material were observed, with a circular shape (Fig. 7). In the post-heat-treated base material, the precipitates, such as γ'' and $M_{23}C_6$, were observed at the grain boundaries. In case of the post-heat-treated stir zone, γ'' and M_6C carbides in the grains were observed, with a circular shape, as shown in Fig. 7. Further, in case of the stir zone after the post heat treatment, more precipitates were formed in the grains than at the grain boundaries due to the higher dislocation density accompanying FSW application.

These precipitates led to the improvement of the mechanical properties such as microhardness and tensile strength. The average Vickers microhardness of the base material and welded zone was 275 and 380 Hv, respectively, as shown in Fig. 8. In the case of the post-heat-treated material, the microhardness significantly increased to 30% as compared to the welded material, which had a distribution of 375 (base material) and 430 Hv (stir zone) on an average, as shown in Fig. 8. Tensile strength also notably increased by the post heat treatment; the tensile strength of the post-heat-treated stir zone specimen was 1475 MPa, which is an increase of more than 50% when compared to the base material, as shown in Fig. 10. Thus, this study shows that the mechanical properties of friction stir welded Inconel 625 alloy are notably improved by precipitates such as γ'' and MC system carbides.

5. Conclusions

FSW can be successfully performed on Inconel 625 alloy at welding speed of 100 mm/min without any defects in the welds. The application of FSW led to a grain refinement from 5 μm to 15 μm in the base material to 1–3 μm in the stir zone; this resulted in the improvement of mechanical properties of the stir zone, wherein microhardness increased by 30% and tensile strength increased by 20% as compared to the base material. After the post heat treatment, precipitates were formed at elevated temperatures, and there was a notable improvement in mechanical properties; microhardness and tensile strength increased by 30% and 50%, respectively, compared to the base material. Thus, the application of the post heat treatment on the friction stir welded Inconel 625 alloy could effectively improve the mechanical properties of the welds.

Acknowledgements

The authors thank Prof. H. Fujii and Mr. Y.D. Jung for performing the heat treatment of the materials.

References

[1] Sims CT, Stoloff NS, Hagel WC. Superalloys. 2nd ed. New York: Wiley-Interscience; 1987.
[2] Kim JD, Kim CJ, Chung CM. Repair welding of etched tubular components of nuclear power plant by Nd:YAG laser. J Mater Process Technol 2001;114:51–6.
[3] Henderson MB, Arrel D, Larsson R, Heobel M, Marchant G. Nickel based superalloy welding practices for industrial gas turbine applications. Sci Technol Weld Join 2004;9:13–21.
[4] Floreen S, Fuch GE, Yang WJ. In: Loria EA, editor. Superalloys 718, 625, 706 and various derivatives. Warrendale (PA): TMS; 1994. p. 13.
[5] Radavich JF, Fort A. In: Loria EA, editor. Superalloys 718, 625, 706 and various derivatives. Warrendale (PA): TMS; 1994. p. 635.
[6] Conder CR, Smith GD, Radavich JF. In: Loria EA, editor. Superalloys 718, 625, 706 and various derivatives. Warrendale (PA): TMS; 1994. p. 447.
[7] Song KH, Fujii H, Nakata K. Effect of welding speed on microstructural and mechanical properties of friction stir welded Inconel 600. Mater Des 2009;30:3972–8.
[8] Song KH, Fujii H, Nakata K. Evaluation of grain refinement and mechanical property on friction stir welded Inconel 600. Mater Trans 2009;50:832–6.
[9] Song KH, Tsumura T, Nakata K. Development of microstructure and mechanical properties in laser-FSW hybrid welded Inconel 600. Mater Trans 2009;50:1832–7.
[10] Howe JM. Interfaces in materials. Wiley-Interscience; 1997.
[11] Humphreys FJ, Hatherly M. Recrystallization and related annealing phenomena. 2nd ed. Elsevier; 2004.
[12] Shankar K, Bhanu Sankara Rao K, Mannan SL. Microstructure and mechanical properties of Inconel 625 superalloy. J Nucl Mater 2001;288:222–32.
[13] Muzyka M. In: Sims CT, Hagel WC, editors. The superalloys. New York: Wiley-Interscience; 1972.
[14] Khan T, Caron P. High temperature materials for power engineering. Part II. Kluwer Academic; 1990.
[15] Curtis RV, Ghosh RN, Mc Lean M. Creep and fracture of engineering materials and structures. London: The Institute of Materials; 1993.